Journal of Neurochemistry, 2007, **101**, 1294–1302 doi:10.1111/j.1471-4159.2007.04525.x

Neurochemical, morphological, and neurophysiological abnormalities in retinas of Sandhoff and GM1 gangliosidosis mice

Christine A. Denny,*[,1] Joseph Alroy,† Basil S. Pawlyk,‡ Michael A. Sandberg,‡ Alessandra d'Azzo§ and Thomas N. Seyfried*

*Biology Department, Boston College, Chestnut Hill, Massachusetts, USA

†Departments of Pathology, Tufts University Schools of Medicine and Veterinary Medicine, and Tufts New England Medical Center, Boston, Massachusetts, USA

‡Berman-Gund Laboratory for the Study of Retinal Degenerations, Harvard Medical School, Massachusetts Eye and Ear Infirmary, Boston, Massachusetts, USA

§Department of Genetics, St. Jude Children's Research Hospital, Memphis, Tennessee, USA

Abstract

Retinal abnormalities are well documented in patients with ganglioside storage diseases. The total content and distribution of retinal glycosphingolipids was studied for the first time in control mice and in Sandhoff disease (SD) and GM1 gangliosidosis mice. Light and electron microscopy of the SD and the GM1 retinas revealed storage in ganglion cells. Similar to previous findings in rat retina, GD3 was the major ganglioside in mouse retina, while GM2 and GM1 were minor species. Total ganglioside content was 44% and 40% higher in the SD and the GM1 retinas, respectively, than in the control retinas. Furthermore, GM2 and GM1 content were 11-fold and 51-fold higher in the SD and the GM1 retinas than in the control retinas, respectively. High concentrations of asialo-GM2 and asialo-GM1 were found in the SD and the GM1 retinas, respectively, but were undetectable in the control retinas. The GSL abnormalities in the SD and the GM1 retinas reflect significant reductions in β-hexosaminidase and β-galactosidase enzyme activities, respectively. Although electroretinograms appeared normal in the SD and the GM1 mice, visual evoked potentials were subnormal in both mutants, indicating visual impairments. Our findings present a model system for assessing retinal pathobiology and therapies for the gangliosidoses.

Keywords: electroretinograms, GA1, GA2, GD3, GM1, GM2, Sandhoff Disease, visual evoked potentials.

J. Neurochem. (2007) **101**, 1294–1302.

Sandhoff disease (SD) and GM1 gangliosidosis are incurable glycosphingolipid (GSL) lysosomal storage diseases caused by genetic deficiencies of lysosomal β-hexosaminidase (*Hexb*) and acid β-galactosidase (β-gal), respectively. SD (a GM2 gangliosidosis) involves the storage of ganglioside GM2 and its asialo derivative GA2 whereas GM1 gangliosidosis involves the storage of ganglioside GM1 and its asialo derivative GA1 in neural and non-neural tissue. The severity of motor and mental dysfunction in the GM2 and the GM1 gangliosidoses correlates with the degree of catabolic enzyme deficiency and with the level of ganglioside storage in the brain leading to either early or late-onset forms of these disorders (Suzuki 1984; Suzuki *et al.* 1995; Gravel *et al.* 1995). In addition, pathological abnormalities have also been found in the retina of SD and GM1 patients that involve membranous cytoplasmic bodies, ganglion cell loss, and optic nerve atrophy (Brownstein *et al.* 1980; Cairns *et al.* 1984). The accumulation of GM2 and GM1 gangliosides in the retinal ganglion cells is greatest in the fovea centralis, producing the characteristic cherry-red spot, surrounded by a

Received October 29, 2006; revised manuscript received December 4, 2006; accepted December 5, 2006.

Address correspondence and reprint requests to Thomas N. Seyfried, Boston College, Biology Department, Chestnut Hill, MA 02467, USA. E-mail: thomas.seyfried@bc.edu

[1]The present address of Christine A. Denny is the Department of Biological Sciences, Columbia University, New York, New York, 10027, USA, cad2125@columbia.edu.

Abbreviations used: CNS, central nervous system; ERGs, electroretinograms; GSLs, glycosphingolipids; *Hexb*, β-hexososaminidase; HPTLC, high-performance thin-layer chromatography; SD, Sandhoff disease; VEPs, visual evoked potentials; β-gal, β-galactosidase.

© 2007 The Authors

white halo in the macula (Kivlin *et al.* 1985). SD patients exhibit optic abnormalities and have visual loss because of impairment of the retinal ganglion cells (Brownstein *et al.* 1980; Norby *et al.* 1980). GM1 patients have visual loss due to GM1 storage in the retinal ganglion cells and have additional mucopolysaccharide storage in the cornea, leading to mild corneal haze (Emery *et al.* 1971; Babarik *et al.* 1976). In general, excessive ganglioside accumulation in these diseases causes neuronal damage or death, inflammation, and progressive neurological deterioration.

Mouse models of SD and GM1 gangliosidosis, deficient in *Hexb* and β-gal activity, respectively, were generated using homologous recombination and embryonic stem cell technology (Sango *et al.* 1995; Hahn *et al.* 1997; Matsuda *et al.* 1997). The *Hexb* −/− mice mimic the pathological, biochemical, and clinical abnormalities of human SD. These mice show severe behavioral abnormalities involving motor coordination and CNS inflammation, and succumb to death at approximately 4.5 months of age. A recent study demonstrated neurite outgrowth abnormalities in the retina of the *Hexb* −/− mice, but no evidence was presented for biochemical or neurophysiological defects (Sango *et al.* 2005). Despite CNS GM1 accumulation from early ages, the β-gal −/− mice do not show behavioral abnormalities until about 6 months of age (Hahn *et al.* 1997; Jeyakumar *et al.* 2003; Hauser *et al.* 2004; Kasperzyk *et al.* 2004, 2005). This differs from the human infantile and the juvenile forms of GM1 gangliosidosis, in which behavioral abnormalities occur early in development. No prior studies have evaluated the content or distribution of gangliosides in retina from normal mice or from lipid storage diseased mice, or have determined whether visual impairments occur in the SD or the GM1 mice.

The electroretinogram (ERG) and visual evoked potential (VEP) are important diagnostic tools used to assess mouse visual electrophysiology (Peachey and Ball 2003). ERGs are used to measure the electrical responses of various cell types in the retina, particularly the ganglion cells, rods, and cones. Whereas the active electrode is placed on the cornea for the ERG, the active electrode is placed on the scalp over the visual cortex for the VEP (Peachey and Ball 2003; Odom *et al.* 2004). The VEP is an important tool for diagnosing the integrity of the visual system (Odom *et al.* 2004). In this study, we investigated for the first time the physiological, morphological, and biochemical abnormalities in the retinas of the SD and the GM1 gangliosidosis mice. This study was designed to evaluate retinal pathobiology in these mutants during the symptomatic stage of the disease in each mutant. This was performed to enhance the probability of finding retinal pathology considering the difficulty in obtaining enough retinal tissue for biochemical analysis. Our results are the first physiological pieces of evidence that show that the retinas of the SD and the GM1 gangliosidosis murine models have neuropathological abnormalities similar to those reported in the retinas of their human counterparts.

Materials and methods

Mice

Sv/129 mice, heterozygous for the *Hexb* gene (hexb +/−), were provided by Dr Richard Proia (National Institutes of Health, Bethesda, MD, USA). B6/129Sv mice, heterozygous for the GM1 β-galactosidase gene (β-gal +/−), were sent to Boston College from Saint Jude Children's Research Hospital, Nashville, TN, USA. These mice were derived by homologous recombination and embryonic stem cell technology as previously described (Sango *et al.* 1995; Hahn *et al.* 1997). The *Hexb* and the β-gal +/− and −/− mice were generated by crossing either −/− or +/− females with −/− males. Specific activities of lysosomal β-hexosaminidase and β-galactosidase in tail snips were used to genotype the SD and the GM1 gangliosidosis mice, respectively, as previously described (Galjaard 1980; Hauser *et al.* 2004). Specific enzyme activities were measured in the retinas of the SD and GM1 mice as well to confirm the gentoypes. All mice were propagated in the Boston College Animal Care Facility and were housed in plastic cages with filter tops containing Sani-Chip bedding (P.J. Murphy Forest Products Corp., Montville, NJ, USA). All mice received PROLAB RMH 3000 chow (LabDiet, Richmond, IN, USA). Water was provided *ad libitum*. The room was maintained at 22°C on a 12 h light – 12 h dark cycle. *Hexb* +/− and −/− mice at 2–4 months of age and β-gal +/− and −/− mice at 6–10 months of age were sacrificed by cervical dislocation. All animal experiments were carried out with ethical committee approval in accordance with the National Institutes of Health Guide for the Care and Use of Laboratory Animals and were approved by the Institutional Animal Care Committee.

Lipid isolation, purification, and quantification

Total lipids were isolated and purified from freeze-dried (lyophilized) retinas using modifications of previously described procedures (Seyfried *et al.* 1978; Hauser *et al.* 2004; Kasperzyk *et al.* 2004). Briefly, the total lipid extract, suspended in solvent A ($CHCl_3$: CH_3OH : H_2O, 30 : 60 : 8 by vol), was applied to a DEAE-Sephadex column (1.2 mL bed vol) equilibrated with solvent A. The column was washed twice with 20 mL of solvent A and the entire neutral lipid fraction, consisting of the initial eluent plus washes, was collected. This fraction contained cholesterol, phosphatidylcholine, phosphatidylethanolamine, plasmologens, ceramide, sphingomyelin, cerebrosides, and asialo gangliosides (GA1 or GA2). The acidic lipids were then eluted from the column with 30 mL of solvent B ($CHCl_3$: CH_3OH : 0.8 mol/L Na acetate, 30 : 60 : 8 by vol). This fraction contained the gangliosides and other acidic lipids to include cardiolipin, phosphatidylserine, phosphatidylinositol, phosphatidic acid, and sulfatides. The gangliosides were isolated and purified from other acidic lipids and analyzed using the resorcinol assay as we previously described (Kasperzyk *et al.* 2004, 2005; Denny *et al.* 2006).

Neutral lipid isolation and purification

GA2 and GA1 were isolated from the neutral lipid fraction as previously described (Kasperzyk *et al.* 2005). A 4 mL aliquot was

© 2007 The Authors
Journal Compilation © 2007 International Society for Neurochemistry,

Table 1 Glycosphingolipid content in retinas of *Hexb* and β-gal mice

Strain	Genotype		Age (months)	N[a]	Ganglioside sialic acid (μg/100 mg dry wt)	NSGLs[b] (μg/100 mg dry wt)	
	Hexb	β-gal				GA2	GA1
Control[c]	+/–	+/–	2–8	3	144 ± 21	–	–
Hexb	–/–		2–4	2	208 (207, 209)	566 (496, 635)	–
β-gal		–/–	6–8	4	201 ± 9*	–	587 ± 19

[a]N, the number of independent samples analyzed. Each sample consisted of approximately 20 retinas.
[b]Determined from densitometric scanning of HPTLC as shown in Fig. 2.
[c]Values represent the mean ± SEM of 3 independent samples from *Hexb* +/– mice and β-gal +/– mice.
*Indicates that the value is significantly different from that of the control mice at $p < 0.05$ as determined from the two-tailed *t*-test.

evaporated under a stream of nitrogen and treated with mild base (1 mL of 0.15 mol/L NaOH) in a shaking water bath at 37°C for 1.5 h. The solution was converted to $CHCl_3$: CH_3OH : dH_2O (8 : 4 : 3 by vol) by addition of 4 mL $CHCl_3$: CH_3OH (2 : 1 by vol) and the Folch partitioning procedure was repeated to separate either GA2 or GA1 from saponified phospholipids. The upper aqueous phase was discarded and the lower organic phase was washed once with 1.72 mL of the Folch 'pure solvent upper phase.' The upper phase was again discarded and the lower phase containing either GA2 or GA1 was evaporated under a stream of nitrogen, re-suspended in 4 mL $CHCl_3$: CH_3OH (2 : 1 by vol), and stored at 4°C.

High-performance thin-layer chromatography

Gangliosides, GA2, and GA1 were analyzed qualitatively by HPTLC according to previously described methods (Ando *et al.* 1978; Seyfried *et al.* 1978; Macala *et al.* 1983; Kasperzyk *et al.* 2004). Lipids were spotted on a 10 × 20 cm Silica gel 60 HPTLC plates (E. Merck, Darmstadt, Germany) using a Camag Linomat III auto-TLC spotter (Camag Scientific Inc., Wilmington, NC, USA). Purified lipid standards were either purchased from Matreya Inc. (Pleasant Gap, PA, USA) or were a gift from Dr Robert Yu (Medical College of Georgia, Augusta, GA, USA). The HPTLC plates were sprayed with either the resorcinol-HCl reagent or the orcinol-H_2SO_4 reagent and heated at 95°C or 100°C for 30 min to visualize gangliosides or neutral glycosphingolipids, respectively (Kasperzyk *et al.* 2005).

The percentage distribution of the glycolipids was determined by scanning the plates on a Personal Densitometer SI with ImageQuant software (Molecular Dynamics, Sunnyvale, CA, USA) for gangliosides or on a ScanMaker 4800 with Scan-Wizard5 v7.00 software (Microtek, Carson, CA, USA) for GA2 and GA1. The density values for GA2 and GA1 were fit to a standard curve of the respective lipid and used to calculate individual concentrations.

Light and electron microscopy

Eyes were immediately fixed with Trump's Fixative (4% formaldehyde and 1% glutaraldehyde in phosphate buffer, pH 7.2), post-fixed in 1% osmium tetroxide in sodium cacodylate buffer for 3 h at 20°C, and then stained en bloc with 5% aqueous uranyl acetate. Specimens were dehydrated in graded ethanol solutions and embedded in Epon-812. Thick sections (1 μm) were stained with toluidine blue (TB) for light microscopy. Thin sections (50–70 nm) were cut in a LKB8801 ultramicrotome, stained with uranyl acetate and lead citrate, and photographed with a Philips EM201 electron microscope. The retinas of the *Hexb* –/– and the β-gal –/– mice were compared with age-matched retinas of the *Hexb* +/– and the β-gal +/– mice, respectively.

Electrophysiological studies

Electroretinograms (ERGs) and visual evoked potentials (VEPs), as a measure of retinal and cortical function, respectively, were

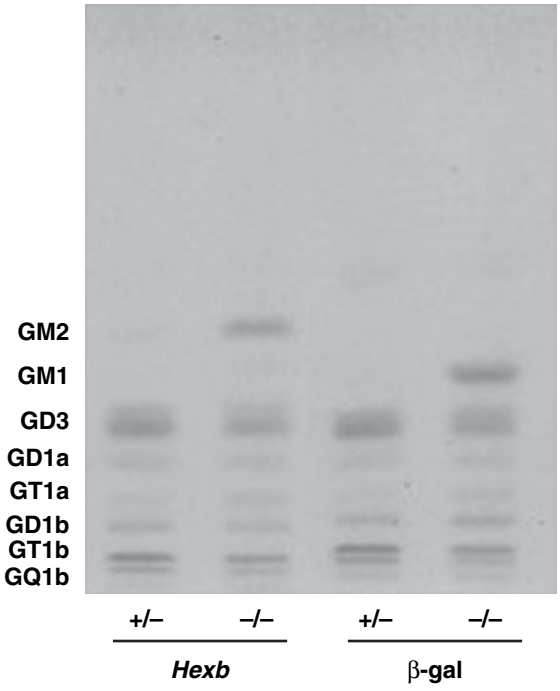

Fig. 1 High-performance thin-layer chromatography of retinal gangliosides in the *Hexb* and the β-gal mice. The amount of ganglioside sialic acid spotted per lane was equivalent to approximately 1.2 μg. The plate was developed by a single ascending run with $CHCl_3$: CH_3OH : dH_2O (55 : 45 : 10, by volume) containing 0.02% $CaCl_2 \cdot 2H_2O$. The bands were visualized with resorcinol-HCl spray.

© 2007 The Authors

Table 2 Ganglioside distribution in retinas of *Hexb* and β-gal Mice[a]

	Genotype			Concentration (μg sialic acid/100 mg dry weight)[b]							
Strain	*Hexb*	β-gal	N[c]	GM3	GM2	GM1	GD3	GD1a	GT1a/LD1	GD1b	GT1b	GQ1b
Control[d]	+/–	+/–	3	5.9 ± 1.7	4.4	1.5 ± 0.1	70.5 ± 8.9	6.7 ± 1.4	1.7 ± 0.5	11.9 ± 1.7	30.8 ± 4.9	15.5 ± 3.6
Hexb	–/–		2	–	52.1 (42.0, 62.3)	3.6 (2.7, 4.6)	70.6 (67.6, 73.7)	11.1 (10.6, 11.6)	9.7 (8.9, 10.5)	13.3 (12.1, 14.5)	33.4 (30.0, 36.7)	14.0 (13.0,15.4)
β-gal		–/–	4	5.1 ± 0.3	–	79.5 ± 3.4*	60.0 ± 3.0	5.7 ± 0.4	5.3 ± 0.6*	14.8 ± 1.1	21.9 ± 1.5	8.4 ± 0.9

[a]Values represent the mean ± SEM.
[b]Determined from densitometric scanning of HPTLC as shown in Fig. 1.
[c]N, the number of independent samples analyzed. Each sample consisted of approximately 20 retinas.
[d]Values represent the mean ± SEM of three independent samples from *Hexb* (+/–) mice and β-gal (+/–) mice.
*Indicates that the value is significantly different from that of the control mice at $p < 0.05$ as determined from the two-tailed *t*-test.

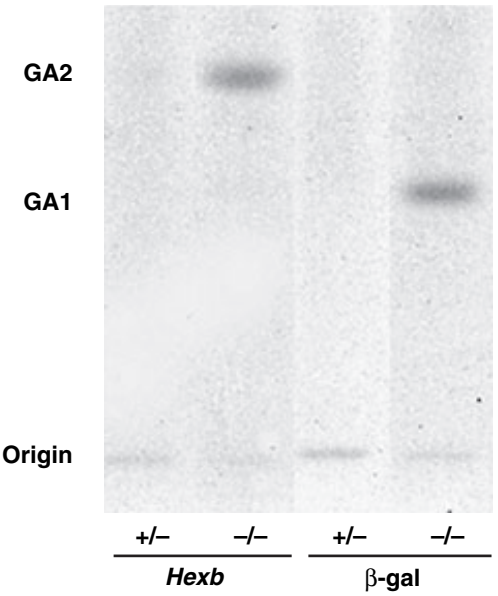

Fig. 2 High-performance thin-layer chromatography of retinal neutral glycosphingolipids in the *Hexb* and the β-gal mice. The amount of lipid spotted per lane was equivalent to approximately 200 μg dry weight. The plate was developed by a single ascending run with $CHCl_3$: CH_3OH : dH_2O (65 : 35 : 8, by vol) containing 0.02% $CaCl_2{\cdot}2H_2O$. The bands were visualized with orcinol-H_2SO_4 spray.

recorded from *Hexb* +/– ($n = 3$) and –/– ($n = 4$) mice at 3.5–4 months of age and from β-gal +/– ($n = 4$) and –/– ($n = 3$) at 6–8 months of age mice. Mice were dark-adapted overnight and anesthetized with ketamine and xylazine (i.p.); one pupil of each animal was topically dilated with phenylephrine hydrochloride and cyclopentolate hydrochloride. Responses were elicited with 10-μs full-field flashes of white light presented every minute at 4.3 log ft.L. for the ERG and every second at 3.4 log ft.L. for the VEP. ERGs were monitored with a silver wire electrode in contact with the cornea, which was anesthetized with proparacaine hydrochloride, and with subdermal electrodes in the neck and the tail as the reference and the ground, respectively. VEPs were monitored with subdermal electrodes in the scalp over the visual cortex as the positive electrode, over the frontal cortex as the reference, and in the tail as the ground following published methods (Ren *et al.* 2000). All responses were differentially amplified at a gain of 1000 (−3db at 2 Hz and 300 Hz; AM502, Tektronix Instruments, Beaverton, OR, USA), digitized at 16-bit resolution over an adjustable peak-to-peak input amplitude (PCI-6251, National Instruments, Austin, TX, USA), and displayed on a personal computer using custom software (Labview, version 7.1, National Instruments). For VEP recordings, consecutive waveforms were averaged ($n = 100$) after suppressing the heart-beat artifact with an adjustable low-pass digital filter (cut-off at 50 Hz) and rejecting waveforms containing movement artifacts by an adjustable voltage window. VEPs can be described as either normal or abnormal, and in some cases, subnormal according to standard criteria in the field (Peachey and Ball 2003; Odom *et al.* 2004).

© 2007 The Authors

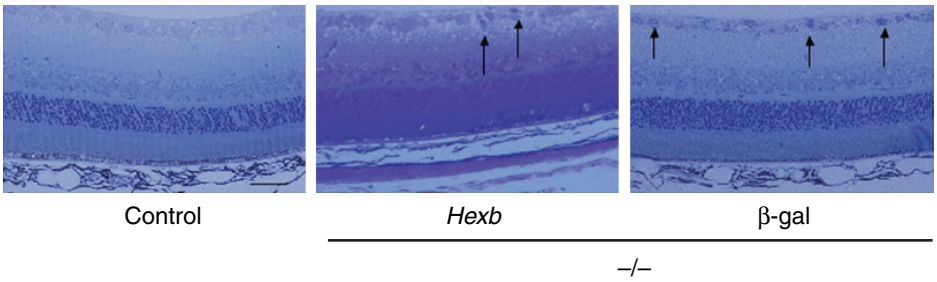

Fig. 3 Toluidine blue staining of retina in the control (*Hexb* +/– and β-gal +/–), the *Hexb* –/–, and the β-gal –/– mice (sagittal, 5 μm). Images shown are at 400× (scale bar: 25 μm). Arrows indicate positive accumulated storage material in the ganglion cell layer.

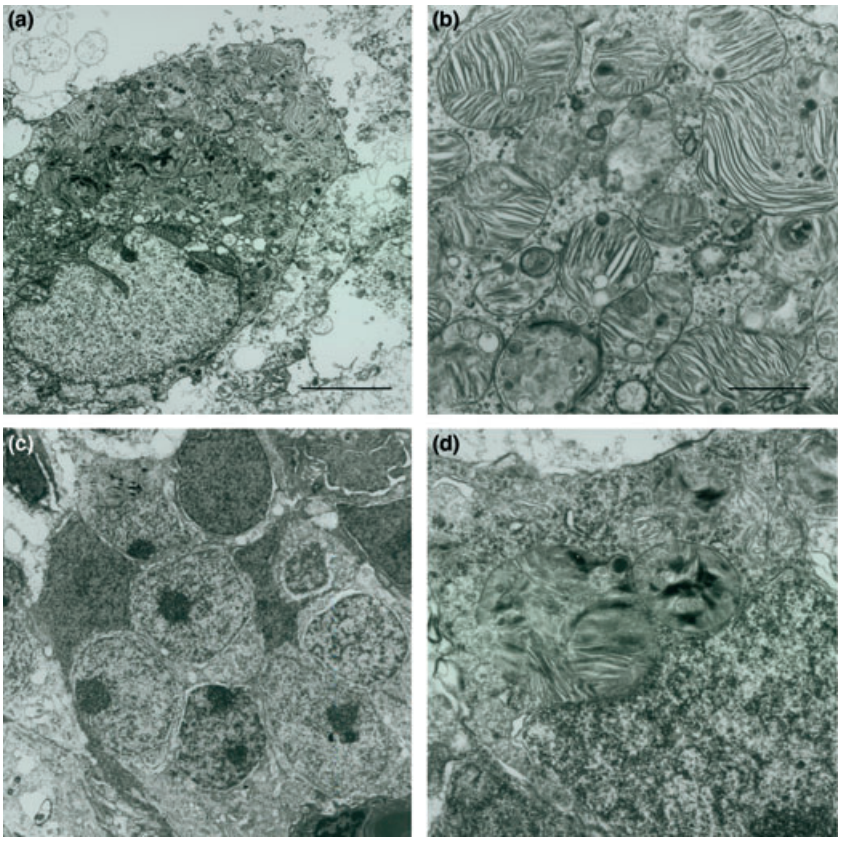

Fig. 4 Low and high magnification electron micrographs of retina of a symptomatic *Hexb* –/– mouse (approximately 4 months of age) illustrating enlarged secondary lysosomes that contain lamellated membrane structures in ganglion cells (a and b), and in the inner nuclear cell layer (c and d). Images shown at 3700× (scale bar: 5 μm) (a and c) and 16 800× (scale bar: 100 μm) (b and d).

Statistical analysis

A two-tailed *t*-test was used to evaluate the significance of differences between the +/– and –/– groups. In each figure, 'n' designates the number of independent samples included in the analysis.

Results

The *Hexb* +/– and the β-gal +/– mice were similar in retinal lipid content, in retinal morphology, and in ERG and VEP responses. Therefore, data for the *Hexb* +/– and the β-gal +/– mice were combined and are presented as a control group (control mice).

Neurochemical abnormalities

The retinal specific activity for hexosaminidase and β-galactosidase in the *Hexb* +/– and the β-gal +/– mice was 14.2 ± 0.4 nmol/mg/h and 10.2 ± 0.6 nmol/mg/h, respectively. In contrast, only residual specific activity was found for these enzymes in the retinas of the *Hexb* –/– mice and the β-gal –/– mice (n = 3–4 independent retinas/group). This reduction in hexosaminidase and β-galactosidase specific activity was associated with significant elevations of total ganglioside content in the retinas of the *Hexb* –/– (44% increase) and the β-gal –/– (40% increase) mice, respectively, when compared to the retinas of the control mice

© 2007 The Authors
Journal Compilation © 2007 International Society for Neurochemistry,

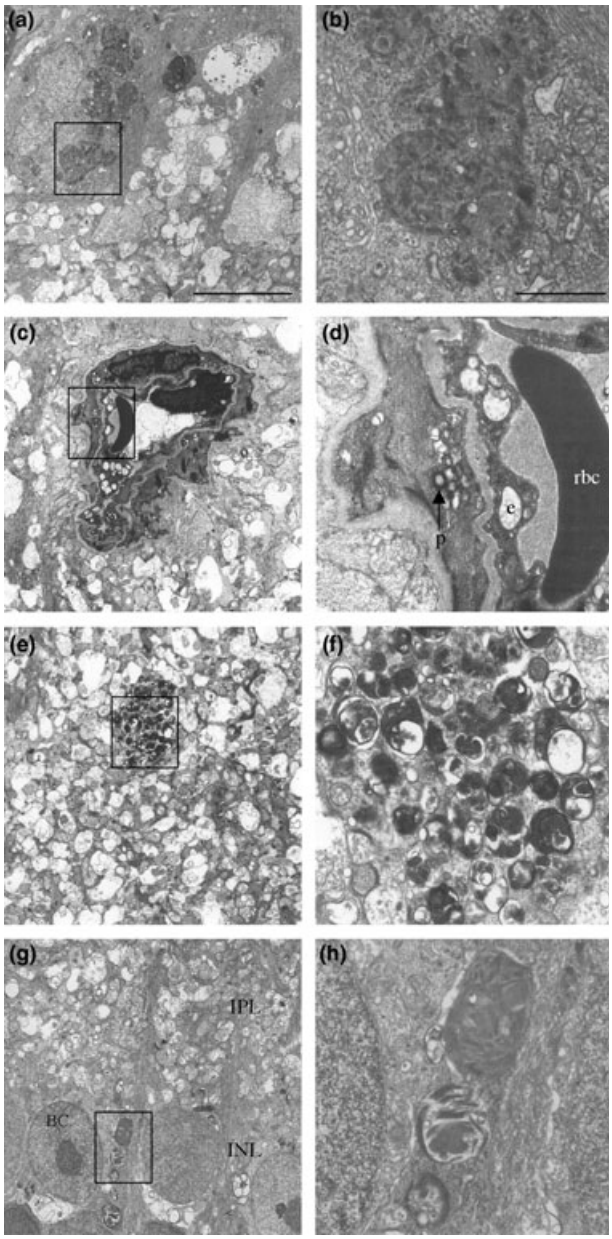

Fig. 5 Electron micrographs of retina of a symptomatic β-gal −/− mouse (approximately 6 months of age). (a and b) Low and high magnification micrographs illustrating enlarged secondary lysosomes packed with lamellated membrane structures in a ganglion cell. (c and d) Low and high magnification micrographs of secondary lysosomes, filled with a few fine fibrillae and few membrane structures, near a blood vessel in the ganglion cell layer containing red blood cells (RBC), endothelial cells (e), and pericytes (p). (e and f) Low and high magnification micrographs of a swollen axon containing spheroids (membrane structures filled with a mixture of lamellated membrane structures) in the inner plexiform layer (IPL). (g and h) Low and high magnification micrograph of secondary lysosomes, which are packed with lamellated membranes structures, within a bipolar cell of the junction between the inner nuclear layer and the IPL revealing bipolar cells that contain relatively small amounts of secondary lysosomes with storage material. Low magnification micrographs were performed at 3700× (scale bar: 5 μm) and high magnification micrographs were performed at 16 800× (scale bar: 100 μm).

(Table 1). The qualitative and quantitative distributions of individual gangliosides in the retinas of the *Hexb* and the β-gal mice are shown in Fig. 1 and Table 2. GD3 was the predominant ganglioside in control mouse retina and comprised 49% of the total distribution. In contrast to the control *Hexb* +/− mice, where GM2 was present in only trace amounts, GM2 was a major ganglioside in the *Hexb* −/− mice (11-fold increase). In the β-gal −/− mice, GM1 was the major ganglioside (51-fold increase), surpassing the content of GD3. The band representing the Purkinje cell enriched gangliosides GT1a/LD1 was noticeably elevated in both the *Hexb* −/− and the β-gal −/− mice. Although gangliosides GT1a and LD1 comigrate on the HPTLC in this solvent system, previous studies showed that LD1 [disialosylparagloboside (disialosyl-nLc4Cer)] is the major ganglioside in this band (Chou *et al.* 1990; Seyfried and Yu 1990). In addition, asialo-GM2 (GA2) and asialo-GM1 (GA1) were elevated in the *Hexb* −/− and the β-gal −/− mice, respectively (Fig. 2 and Table 1). These findings indicate that reductions in lysosomal enzyme activity in the retinas are associated with significant changes in glycosphingolipid content and distribution.

Light and electron microscopy

Light microscopy examination of the retina revealed the accumulation of storage material in the ganglion cell layer of the *Hexb* −/− and the β-gal −/− mice (Fig. 3). The number of affected ganglion cells appear greater in the β-gal −/− mice than in the *Hexb* −/− mice. Storage material was not present in the ganglion cells in the retinas of the control mice. Electron microscopic examinations in the *Hexb* −/− mice revealed large secondary lysosomes filled with lamellated membrane structures (i.e., zebra bodies) in the ganglion cells (Figs 4a and b) and large secondary lysosomes packed with zebra bodies in the inner nuclear cell layer (Figs 4c and d).

Electron microscopic examinations in the β-gal −/− mice revealed enlarged secondary lysosomes packed with lamellated membrane structures (Figs 5a and b), and multiple, small vacuoles (i.e., secondary lysosomes), containing fine fibrillar material in endothelial cells and in pericytes (Figs 5c and d). In addition, enlarged axons, containing spheroids, were present in the inner plexiform layer (IPL) (Figs 5e and 5f). A relatively small number of secondary lysosomes with lamellated membranes were present in the inner nuclear layer (INL) (Figs 5g and 5 h).

Electroretinograms and visual evoked potentials

Figure 6 shows the representative ERGs and VEPs from the *Hexb* and the β-gal mice. The ERGs were consistently

© 2007 The Authors

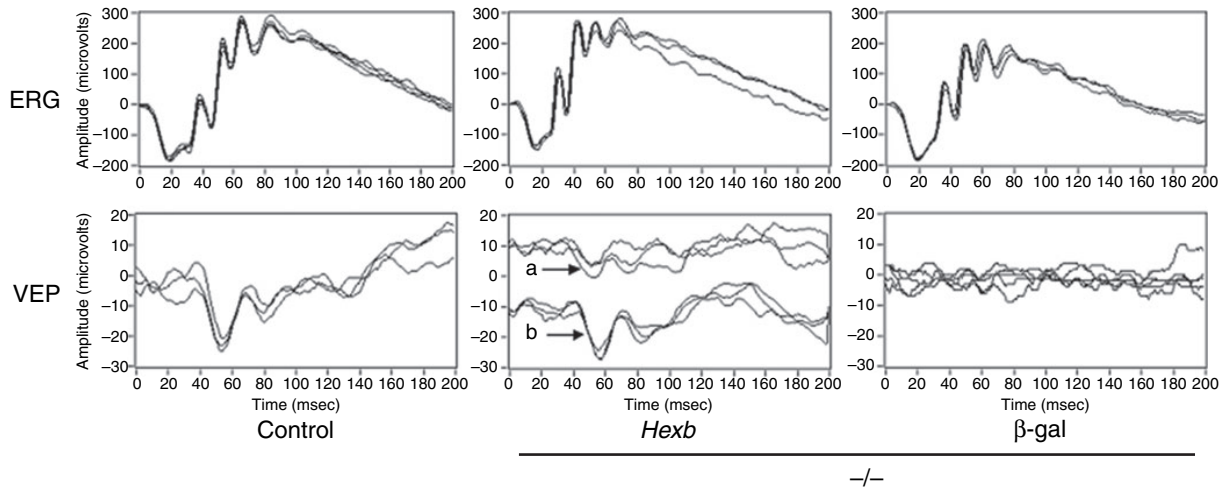

Fig. 6 Electroretinograms and visual evoked potentials of control (*Hexb* +/– and β-gal +/–), *Hexb* –/–, and β-gal –/– mice. Each panel shows three or more responses to illustrate reproducibility, and the lower middle panel shows responses from two animals to illustrate that responses could range from normal (b) to subnormal (a) in the *Hexb* –/– mice.

normal in all of the *Hexb* and the β-gal mice. VEPs recorded from the *Hexb* +/– and the β-gal +/– mice were also consistently normal. In contrast, VEPs recorded from *Hexb* –/– mice ranged from normal to subnormal, suggesting variable visual loss (indicated by arrows a and b). In addition, all VEPs were abnormal in the β-gal –/– mice, suggesting greater visual impairment.

Discussion

Our findings show that deficiencies in lysosomal hexosaminidase and β-galactosidase enzyme activities were associated with abnormalities in retinal glycosphingolipid composition, subcellular morphology, and visual function in the *Hexb* –/– and in the β-gal –/– mice, respectively. In contrast to control mice, where GM2 and GM1 were present in trace amounts, GM2 and GM1 were greatly elevated in the *Hexb* –/– and the β-gal –/– mice, respectively. The storage of GM1 in the β-gal –/– mice (51-fold) was greater than the storage of GM2 in the *Hexb* –/–mice (11-fold). The degree of GM2 storage in the retina of the *Hexb* –/– mice was less than that found previously in brain tissue from these mice (Denny *et al.* 2006). In contrast, the degree of GM1 storage in the retina of the β-gal –/– mice greatly exceeded that in the brain tissue from these mice (approximately 11-fold) (Hauser *et al.* 2004). As the storage of asialo-GM1 in the β-gal –/– mice (587 μg /100 mg dry wt.) was similar to the storage of asialo-GM2 in the *Hexb* –/– mice (566 μg/100 mg dry wt.), we suggest the greater visual impairment in the β-gal –/– mice than in the *Hexb* –/– mice is due primarily to differences in degree of ganglioside storage. As the ganglioside storage occurs for a longer period of time in the β-gal –/– mice (6–8 months) than in the *Hexb* –/– mice (3–4 months), our findings also support the possibility of a time- and storage (GM2, GM1)-dependent degeneration in these retinas (Sango *et al.* 2005). Further studies will be needed to test this possibility.

The retina is unique among mature mammalian CNS tissues in expressing high concentrations of ganglioside GD3 (Holm *et al.* 1972; Seyfried *et al.* 1982a,b; Graus *et al.* 1984). GD3 is pro-angiogenic, evolutionary conserved, and enriched in tissues with high metabolic activity like that of the retina (Seyfried and Yu 1985; Ziche *et al.* 1992; Irvine and Seyfried 1994). Although GD3 content was largely unaffected in the *Hexb* –/– and the β-gal –/– mice, the content of LD1 was increased in association with GM2 and GM1 storage in these mutants, respectively. LD1 is enriched in Purkinje cells and is significantly reduced in the cerebellums of the nervous and the Purkinje cell degeneration (PCD) mutant mice (Seyfried *et al.* 1982a,b; Seyfried *et al.* 1987; Chou *et al.* 1990 Seyfried and Yu 1990). Interestingly, these mice also express retinal degeneration and visual impairment (Mullen *et al.* 1976; Ren *et al.* 2000; Chang *et al.* 2002). We suggest that the elevation of retinal LD1 in the storage disease mice may be a compensatory response to the visual impairment and that LD1 may play a role in retinal function. Further studies, possibly analyzing retinal ganglioside content of the nervous and the PCD mutant mice, will be necessary to elucidate this possibility.

Morphological examination of retinas of SD and GM1 gangliosidosis patients often show large numbers of concentric membranous bodies interspersed with zebra bodies in retinal ganglion cells. These bodies are formed from spontaneous aggregation of glycosphingolipids (Harcourt and Dobbs 1968; Alroy *et al.* 1991). We found similar morphological abnormalities in the retinal ganglion cells in the *Hexb* –/– and the β-gal –/– mice. However, the number

© 2007 The Authors
Journal Compilation © 2007 International Society for Neurochemistry,

of affected ganglion cells storing glycosphingolipids appeared to be greater in the β-gal −/− mice than in the *Hexb* −/− mice. In contrast to human SD, where a prominent cherry-red spot is consistently seen in the retina, the *Hexb* −/− mice did not show the characteristic cherry-red spot (Sango *et al.* 2005).

Ophthalmologic examinations of SD and GM1 gangliosidosis patients often show abnormalities in VEPs, consistent with visual impairment or blindness (Cairns *et al.* 1984; Gravel *et al.* 1995). ERGs, however, are generally normal in patients with SD and GM1 gangliosidosis. Electrophysiological abnormalities have also been described in cats and dogs with GM1 gangliosidosis, and in cats with α-mannosidosis (Murray *et al.* 1977; Alroy *et al.* 1991, 1992). Our results provide the first evidence for visual impairment in the *Hexb* −/− and the β-gal −/− mice. Although the ERGs were normal in the *Hexb* and the β-gal mice, demonstrating normal outer retinal function, the VEPs were consistently abnormal in the β-gal −/− mice and were variably reduced in the *Hexb* −/− mice. Variations in VEPs in the *Hexb* −/− mice may be due to variations in total GSL storage, age of onset, and number of affected ganglion cells.

In summary, our results show that significant reductions in retinal lysosomal β-hexosaminidase and β-galactosidase enzyme activities result in GSL abnormalities in the retinas of the *Hexb* −/− and the β-gal −/− mice and are associated with membranous cytoplasmic bodies and altered retinal architecture. Furthermore, we demonstrate for the first time that retinal ganglioside storage produces visual impairments in the *Hexb* −/− and the β-gal −/− mice. We suggest that the retina may be a new model system for assessing retinal pathobiology and new therapies for the gangliosidoses.

Acknowledgments

The authors would like to acknowledge the late Dr Grant Balkema for his helpful discussions of this work. We also thank Jason R. Chalifoux, Youngho P. Kim, Inna Lomakina, and Gregory Gressel for technical assistance. The work was supported in part by NIH grants HD39722, RO1-DK52025, and EYO16350, the Boston College Research Expense Fund, the National Tay-Sachs and Allied Disease Association Inc. (NTSAD), and the Foundation Fighting Blindness.

References

Alroy J., Bachrach A., Thalhammer J. G., Panjwani N., Richard R., DeGasperi R., Warren C. D., Albert D. M. and Raghavan S. S. (1991) Clinical, neurophysiological, biochemical and morphological features of eyes in Persian cats with mannosidosis. *Virchows Archiv. B Cell. Pathol.* **60**, 173–180.

Alroy J., Orgad U., DeGasperi R., Richard R., Warren C. D., Knowles K., Thalhammer J. G. and Raghavan S. S. (1992) Canine GM1-gangliosidosis. A clinical, morphologic, histochemical, and biochemical comparison of two different models. *Am. J. Pathol.* **140**, 675–689.

Ando S., Chang N. C. and Yu R. K. (1978) High-performance thin-layer chromatography and densitometric determination of brain ganglioside compositions of several species. *Anal. Biochem.* **89**, 437–450.

Babarik A., Benson P. F. and Fensom A. H. (1976) Corneal clouding in GM1-generalized gangliosidosis. *Br. J. Ophthalmol.* **60**, 565–567.

Brownstein S., Carpenter S., Polomeno R. C. and Little J. M. (1980) Sandhoff's Disease (GM2 Gangliosidosis Type 2). *Arch. Ophthalmol.* **98**, 1089–1097.

Cairns L. J., Green W. R. and Singer H. S. (1984) GM1 Gangliosidosis, type 2: ocular clinicopathologic correlation. *Graefe's Arch. Clin. Exp. Ophthalmol.* **222**, 51–62.

Chang B., Hawes N. L., Hurd R. E., Davisson M. T., Nusinowitz S. and Heckenlively J. R. (2002) Retinal degeneration mutants in the mouse. *Vision Res.* **42**, 517–525.

Chou D. K., Flores S. and Jungalwala F. B. (1990) Identification of disialosyl paragloboside and O-acetyldisialosyl paragloboside in cerebellum and embryonic cerebrum. *J. Neurochem.* **54**, 1598–607.

Denny C. A., Kasperzyk J. L., Gorham K. N., Bronson R. T. and Seyfried T. N. (2006) Influence of caloric restriction on motor behavior, longevity, and brain lipid composition in Sandhoff disease mice. *J. Neurosci. Res.* **83**, 1028–38.

Emery J. M., Green W. R., Wyllie R. G. and Howell R. R. (1971) *GM1-gangliosidosis. Ocular and pathological manifestations*. *Arch. Opthalmol.***85**, 177–187.

Galjaard H. (1980) *Genetic Metabolic Disease: Diagnosis and Prenatal Analysis*. pp. 82–121. Elsevier Science, Amsterdam.

Graus F., Cordon-Cardo C., Houghton A. N., Melamed M. R. and Old L. J. (1984) Distribution of the ganglioside GD3 in the human nervous system detected by R24 mouse monoclonal antibody. *Brain Res.* **324**, 190–4.

Gravel R. A., Clarke J. T. R., Kaback M. M., Mahuran D., Sandhoff K. and Suzuki K. (1995) The GM2 gangliosidoses, in *The Metabolic and Molecular Bases of Inherited Disease* ,7th Edn (Scriver C. R., Beaudet A. L., Sly W. S. and Valle D., eds.), Vol. 2, pp. 2839–2879. McGraw-Hill, Inc., New York.

Hahn C. N., del Pilar Martin M., Schroder M., Vanier M. T., Hara Y., Suzuki K., Suzuki K. and d'Azzo A. (1997) Generalized CNS disease and massive GM1-ganglioside accumulation in mice defective in lysosomal acid beta-galactosidase. *Hum. Mol. Genet.* **6**, 205–211.

Harcourt R. B. and Dobbs R. H. (1968) Ultrastructure of the retina in Tay-Sach's disease. *Br. J. Ophthalmol.* **52**, 898–902.

Hauser E. C., Kasperzyk J. L., d'Azzo A. and Seyfried T. N. (2004) Inheritance of lysosomal acid β-galactosidase activity and gangliosides in crosses of DBA/2J and knockout mice. *Biochem. Genet.* **42**, 241–257.

Holm M., Mansson J. E., Vanier M. T. and Svennerholm L. (1972) Gangliosides of human, bovine, and rabbit retina. *Biochim. Biophys. Acta* **280**, 356–364.

Irvine R. A. and Seyfried T. N. (1994) Phylogenetic conservation of ganglioside GD3 expression during early vertebrate ontogeny. *Comp. Biochem. Physiol. B Biochem. Mol. Biol.* **109**, 603–612.

Jeyakumar M., Thomas R., Elliot-Smith E., Smith D. A., van der Spoel A. C., d'Azzo A., Perry V. H., Butters T. D., Dwek R. A. and Platt F. M. (2003) Central nervous system inflammation is a hallmark of pathogenesis in mouse models of GM1 and GM2 gangliosidosis. *Brain* **126**, 974–987.

Kasperzyk J. L., El-Abbadi M. M., Hauser E. C., D'Azzo A., Platt F. M. and Seyfried T. N. (2004) *N*-butyldeoxygalactonojirimycin reduces neonatal brain ganglioside content in a mouse model of GM1 gangliosidosis. *J. Neurochem.* **89**, 645–653.

© 2007 The Authors
Journal Compilation © 2007 International Society for Neurochemistry,

Kasperzyk J. L., d'Azzo A., Platt F. M., Alroy J. and Seyfried T. N. (2005) Substrate reduction therapy reduces ganglioside content in postnatal cerebrum-brainstem and cerebellum in a mouse model of GM1 gangliosidosis. *J. Lipid Res.* **46**, 744–751.

Kivlin J. D., Sanborn G. E. and Myers G. G. (1985) The cherry-red spot in Tay-Sachs and other storage diseases. *Ann. Neurol.* **17**, 356–360.

Macala L. J., Yu R. K. and Ando S. (1983) Analysis of brain lipids by high performance thin-layer chromatography and densitometry. *J. Lipid Res.* **24**, 1243–1250.

Matsuda J., Suzuki O., Oshima A. *et al.* (1997) Beta-galactosidase-deficient mouse as an animal model for GM1-gangliosidosis. *Glycoconj. J.* **14**, 729–736.

Mullen R. J., Eicher E. M. and Sidman R. L. (1976) Purkinje cell degeneration, a new neurological mutation in the mouse. *Proc. Nat Acad. Sci.* **73**, 208–212.

Murray J. A., Blakemore W. F. and Barnett K. C. (1977) Ocular lesions in cats with GM1-gangliosidosis with visceral involvement. *J. Small Anim. Pract.* **18**, 1–10.

Norby S., Jensen O. A. and Schwartz M. (1980) Retinal and cerebellar changes in early fetal Sandhoff disease (GM2-gangliosidosis type 2). *Metab. Pediatr. Ophthalmol.* **4**, 115–119.

Odom J. V., Bach M., Barber C., Brigell M., Marmor M. F., Tormene A. P., Holder G. E. and Vaegan. (2004) Visual evoked potentials standard. *Documenta Ophthalmol.* **108**, 115–123.

Peachey N. S. and Ball S. L. (2003) Electrophysiological analysis of visual function in mutant mice. *Documenta Ophthalmol.* **107**, 13–36.

Ren J. C., LaVail M. M. and Peachey N. S. (2000) Retinal degeneration in the nervous mutant mouse. III. Electrophysiological studies of the visual pathway. *Exp. Eye Res.* **70**, 467–473.

Sango K., Yamanaka S., Hoffmann A. *et al.* (1995) Mouse models of Tay-Sachs and Sandhoff diseases differ in neurologic phenotype and ganglioside metabolism. *Nat. Genet.* **11**, 170–176.

Sango K., Takano M., Ajiki K., Tokashiki A., Arai N., Kawano H., Horie H. and Yamanaka S. (2005) Impaired neurite outgrowth in the retina of a murine model of Sandhoff disease. *Invest. Ophthalmol. Vis. Sci.* **46**, 3420–3425.

Seyfried T. N. and Yu R. K. (1985) Ganglioside GD3: structure, cellular distribution, and possible function. *Mol. Cell Biochem.* **68**, 3–10.

Seyfried T. N. and Yu R. K. (1990) Cerebellar Ganglioside Abnormalities in *pcd* Mutant Mice. *J. Neurosci. Res.* **26**, 105–111.

Seyfried T. N., Glaser G. H. and Yu R. K. (1978) Cerebral, cerebellar, and brain stem gangliosides in mice susceptible to audiogenic seizures. *J. Neurochem.* **31**, 21–27.

Seyfried T. N., Yu R. K., Miyazawa N. and Lai Y-L. (1982a) Retinal gangliosides in RCS mutant rats. *J. Neurochem.* **39**, 277–279.

Seyfried T. N., Yu R. K. and Miyazawa N. (1982b) Differential cellular enrichment of gangliosides in the mouse cerebellum: analysis using neurological mutants. *J. Neurochem.* **38**, 551–559.

Seyfried T. N., Bernard D. J. and Yu R. K. (1987) Effect of Purkinje cell loss on cerebellar gangliosides in nervous mutant mice. *J. Neurosci. Res.* **17**, 251–255.

Suzuki K. (1984) Gangliosides and disease: a review. *Trans. Exp. Med. Biol.* **174**, 407–418.

Suzuki Y., Sakuraba H. and Oshima A. (1995) β-Galactosidase deficiency (β-galactosidosis): GM1 gangliosidosis and Morquio B disease, in *The Metabolic and Molecular Bases of Inherited Disease* (Scriver C. R., Beaudet A. L., Sly W. S. and Valle D., eds.), pp. 2785–2823. McGraw-Hill Inc, New York.

Ziche M., Morbidelli L., Alessandri G. and Gullino P. M. (1992) Angiogenesis can be stimulated or repressed *in vivo* by a change in GM3:GD3 ganglioside ratio. *Lab. Invest.* **67**, 711–715.

© 2007 The Authors
Journal Compilation © 2007 International Society for Neurochemistry,